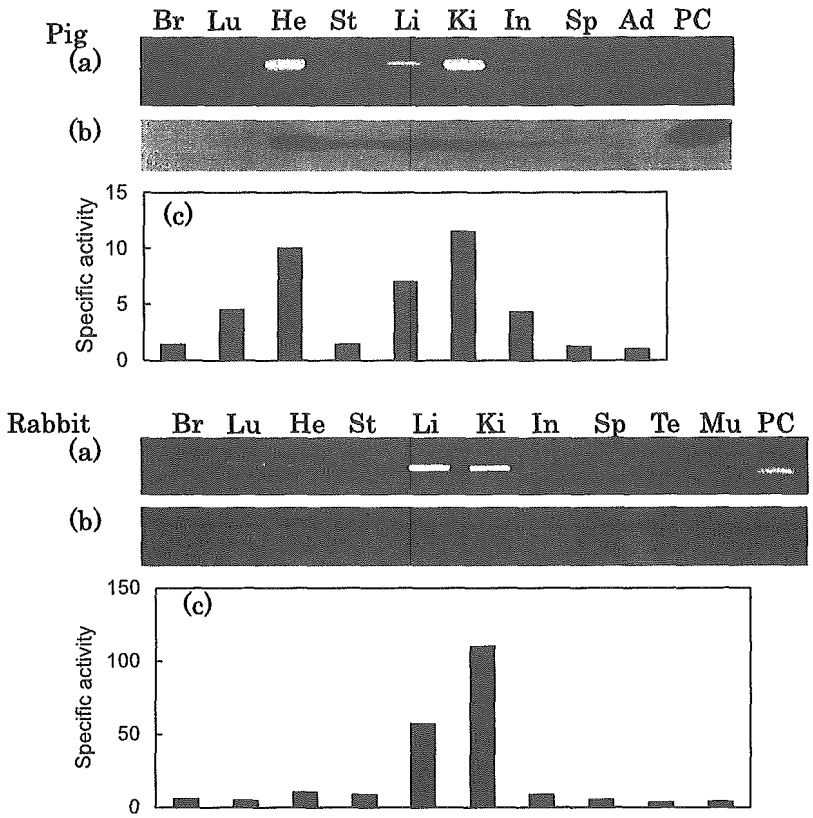

Fig. 2. Distribution of tetrameric CR and its mRNA in pig and rabbit tissues. (a) RT-PCR analysis of expression of mRNAs for PHCR and RaCR. (b) Western blot using the anti-rPHCR antibody, in which the 0.5 M NaCl extracts of rabbit (20 μg protein) and rabbit (40 μg protein) were analyzed. (c) Activity analysis. 4-Benzoylpyridine and 4-hexanoylpyridine were used as the substrates of the enzymes of pig and rabbit, respectively, and the values represent the means (mU/mg) of the two experiments. Tissues: Br, brain; Lu, lung; He, heart; St, stomach; Li, liver; Ki, kidney; In, small intestine; Sp, spleen; Ad, adrenal gland; Te, testis; and Mu, muscle. Positive control (PC): cDNAs for PHCR and NDRD, rPHCR (10 ng) and rNDRD (1 μg).

which have not been characterized enzymologically. The present study also reveals that rabbit NDRD is identical to RaCR, which was the same enzyme species as PHCR. Both PHCR and RaCR were distributed in many tissues of the two species, with liver and kidney showing high expression levels of the enzymes. Although tetrameric CR or NDRD has not been studied in pig tissues, an oligomeric CR (F4 in Ref. [17]) and tetrameric NDRD with CR activity [21] have been purified from rabbit liver. The N-terminal sequence of the rabbit liver NDRD [21] clearly differs from that of RaCR, which suggests the existence of at least two distinct NDRDs with CR activity in animal tissues. However, our on-going characterization of the rabbit liver CR and NDRD suggests that F4 is the only oligomeric form of CR with NDRD activity and is functionally identical to RaCR characterized here (M. Nagano, A. Hara, unpublished results). Moreover, the substrate specificity of RHCR and RaCR for the alkyl phenyl ketones, together with the reversibility of the reaction and pH dependency, resembles the properties of dog liver CR [18]. Re-examination of the properties of dog liver CR and its cDNA cloning show that the dog enzyme is structurally and functionally similar

to PHCR and RaCR (M. Nagano, S. Ishikura, unpublished results). Therefore, the tetrameric form of CR may exist in tissues of many mammals.

Among the substrates of PHCR and RaCR, isatin, 16-ketoestrone and retinals are endogenous. The V_{max}/K_m values for isatin that were determined with PHCR and RaCR at pH 7.4 are low compared to that of human monomeric CR [6], but are higher than those of L-xylulose reductase [26] and several enzymes in the aldo–keto reductase family [27]. The V_{max}/K_m values for 16-ketoestrone are also higher than those of the enzymes of the aldo–keto reductase family [27]. The ability to reduce retinals is a unique characteristic of PHCR and RaCR, because CRs possessing retinal reductase activity have not been reported previously. The K_m and V_{max}/K_m values of the enzymes for all-*trans*-retinal are comparable or superior to those reported with isoenzymes (or isoforms) of microsomal retinol dehydrogenase and cytosolic alcohol dehydrogenase in mammalian tissues [28,29]. Therefore, the tetrameric form of CR may act as one of the reductases for endogenous carbonyl compounds at least in pig and rabbit tissues.

The sequences of PHCR, rabbit NDRD (i.e., RaCR) and human PSCD comprise a C-terminal PTS1-like tripeptide, SRL (Fig. 1). Human PSCD has been shown to be a peroxisomal protein [19]. The present immunofluorescence study of the expressed PHCR in HeLa cells demonstrated that the SRL tripeptide in the enzyme sequence also acts as a peroxisomal targeting signal for this enzyme. Since PHCR and RaCR were extracted and purified as the soluble forms from the tissues, the enzymes probably reside within the peroxisome matrix of the cells and easily leak out from the organelle during homogenization. In this respect, PHCR and RaCR are different from the previously known monomeric and tetrameric CRs, which are localized in the mitochondria, endoplasmic reticula and/or cytosol of mammalian cells [1]. Recently, a peroxisomal isoenzyme of $NADP^+$-dependent isocitrate dehydrogenase has been suggested to provide the intraperoxisomal supply of NADPH [30]. Therefore, we propose that mammalian peroxisomes containing the NADPH-dependent tetrameric CR are responsible for the metabolism of endogenous isatin, estrogen and vitamin A, as well as xenobiotic carbonyl compounds.

Acknowledgements

This work was supported by a grant (to N. Usami) for encouragement of young scientists from the Gifu Pharmaceutical University.

References

[1] G.L. Forrest, B. Gonzalez, Carbonyl reductase, Chem. Biol. Interact. 129 (2000) 21–40.
[2] B. Wermuth, K.M. Bohren, G. Heinemann, J.-P. von Wartburg, K.H. Gabbay, Human carbonyl reductase. Nucleotide sequence analysis of a cDNA and amino acid sequence of the encoded protein, J. Biol. Chem. 263 (1988) 16185–16188.
[3] M. Tanaka, S. Ohno, S. Adachi, S. Nakajin, M. Shinoda, Y. Nagahama, Pig testicular 20β-hydroxysteroid dehydrogenase exhibits carbonyl reductase-like structure and activity, J. Biol. Chem. 267 (1992) 13451–13455.
[4] B. Gonzalez, A. Sapra, H. Rivera, W.D. Kaplan, B. Yam, G.L. Forrest, Cloning and expression of the cDNA encoding rabbit liver carbonyl reductase, Gene 154 (1995) 297–298.
[5] H. Jörnvall, B. Persson, M. Krook, S. Atrian, R. Gonzàlez-Duarte, J. Jeffery, D. Ghosh, Short-chain dehydrogenases/reductases (SDR), Biochemistry 34 (1995) 6003–6013.
[6] N. Usami, K. Kitahara, S. Ishikura, M. Nagano, S. Sakai, A. Hara, Characterization of a major form of human isatin reductase and the reduced metabolite, Eur. J. Biochem. 268 (2001) 5755–5763.
[7] T. Nakayama, K. Yashiro, Y. Inoue, K. Matsuura, H. Ichikawa, A. Hara, H. Sawada, Characterization of pulmonary carbonyl reductase of mouse and guinea pig, Biochim. Biophys. Acta 882 (1986) 220–227.
[8] H. Oritani, Y. Deyashiki, T. Nakayama, A. Hara, H. Sawada, K. Matsuura, Y. Bunai, I. Ohya, Purification and characterization of pig lung carbonyl reductase, Arch. Biochem. Biophys. 292 (1992) 539–547.
[9] K. Matsuura, Y. Bunai, I. Ohya, A. Hara, M. Nakanishi, H. Sawada, Ultrastructural localization of carbonyl reductase in mouse lung, Histochem. J. 26 (1994) 311–316.
[10] S. Ishikura, N. Usami, K. Kitahara, T. Isaji, K. Oda, J. Nakagawa, A. Hara, Enzymatic characteristics and subcellular distribution of a short-chain dehydrogenase/reductase family protein, P26h, in hamster testis and epididymis, Biochemistry 40 (2001) 214–224.

[11] M. Nakanishi, Y. Deyashiki, T. Nakayama, K. Sato, A. Hara, Cloning and sequence analysis of a cDNA encoding tetrameric carbonyl reductase of pig lung, Biochem. Biophys. Res. Commun. 194 (1993) 1311–1316.
[12] M. Nakanishi, Y. Deyashiki, K. Ohshima, A. Hara, Cloning, expression and tissue distribution of mouse tetrameric carbonyl reductase. Identity with an adipocyte 27-kDa protein, Eur. J. Biochem. 228 (1995) 381–387.
[13] U.C.T. Oppermann, K.J. Netter, E. Maser, Cloning and primary structure of murine 11β-hydroxysteroid dehydrogenase/microsomal carbonyl reductase, Eur. J. Biochem. 227 (1995) 202–208.
[14] Y. Imamura, K. Iwamoto, Y. Yanachi, T. Higuchi, M. Otagiri, Postnatal development, sex-related differences and hormonal regulation of acetohexamide reductase activities in rat liver and kidney, J. Pharmacol. Exp. Ther. 264 (1993) 166–171.
[15] H. Takada, M. Otagiri, Y. Imamura, 20β-Hydroxysteroid dehydrogenase catalyzes ketone-reduction of acetohexamide, an oral antidiabetic drug, in liver microsomes of adult male rats, J. Pharmacol. Exp. Ther. 287 (1998) 504–507.
[16] Y. Imamura, T. Migita, M. Otagiri, T. Choshi, S. Hibino, Purification and catalytic properties of a tetrameric carbonyl reductase from rabbit heart, J. Biochem. (Tokyo) 125 (1999) 41–47.
[17] A. Hara, T. Nakayama, Y. Deyashiki, K. Kariya, H. Sawada, Carbonyl reductase of dog liver: purification, properties and kinetic mechanism, Arch. Biochem. Biophys. 244 (1986) 238–247.
[18] H. Sawada, A. Hara, T. Nakayama, F. Kato, Reductases for aromatic aldehydes and ketones from rabbit liver. Purification and characterization, J. Biochem. (Tokyo) 87 (1980) 1153–1165.
[19] M. Fransen, P.P. Van Veldhoven, S. Subramani, Identification of peroxisomal proteins by using M13 phage protein VI phage display: molecular evidence that mammalian peroxisomes contain a 2,4-dienoyl-CoA reductase, Biochem. J. 340 (1999) 561–568.
[20] X. Parés, P. Julià, Isoenzymes of alcohol dehydrogenase in retinoid metabolism, Methods Enz. 189 (1990) 436–441.
[21] D.-Y. Huang, Y. Ichikawa, Purification and characterization of a novel cytosolic NADP(H)-dependent retinol oxidoreductase from rabbit liver, Biochim. Biophys. Acta 1338 (1997) 47–59.
[22] N. Tanaka, T. Nonaka, K.T. Nakamura, A. Hara, SDR: structure, mechanism of action and substrate recognition, Cur. Org. Chem. 5 (2001) 89–111.
[23] Y. Imamura, T. Migita, M. Anraku, M. Otagiri, Inhibition of rabbit heart carbonyl reductase by fatty acids, Biol. Pharm. Bull. 22 (1999) 731–733.
[24] Y. Imamura, T. Migita, Y. Uriu, M. Otagiri, T. Okawara, Inhibitory effects of flavonoids on rabbit heart carbonyl reductase, J. Biochem. (Tokyo) 127 (2000) 653–658.
[25] S.J. Gould, G.-A. Keller, N. Hosken, J. Wilkinson, S. Subramani, A conserved tripeptide sorts proteins to peroxisomes, J. Cell Biol. 108 (1989) 1657–1664.
[26] J. Nakagawa, S. Ishikura, J. Asami, T. Isaji, N. Usami, A. Hara, T. Sakurai, K. Tsuritani, K. Oda, M. Takahashi, M. Yoshimoto, N. Otsuka, K. Kitamura, Molecular characterization of mammalian dicarbonyl/L-xylulose reductase and its localization in kidney, J. Biol. Chem. 277 (2002) 17883–17891.
[27] T. O'Connor, L.S. Ireland, D.J. Harrison, J.D. Hayes, Major differences exist in the function and tissue-specific expression of human aflatoxin B_1 aldehyde reductase and the principal human aldo–keto reductase AKR1 family members, Biochem. J. 343 (1999) 487–504.
[28] W.S. Blaner, R. Piantedosi, A. Sykes, S. Vogel, Retinoic acid synthesis and metabolism, in: H. Nau, W.S. Blaner (Eds.), Retinoids: The Biochemical and Molecular Basis of Vitamin A and Retinoid Action, Springer, Berlin, 1999, pp. 117–149.
[29] G. Duester, Families of retinoid dehydrogenases regulating vitamin A function. Production of visual pigment and retinoic acid, Eur. J. Biochem. 267 (2000) 4315–4324.
[30] T. Yoshihara, T. Hamamoto, R. Munakata, R. Tajiri, M. Ohsumi, S. Yokota, Localization of cytosolic NADP-dependent isocitrate dehydrogenase in the peroxisomes of rat liver cells: biochemical and immunochemical studies, J. Histochem. Cytochem. 49 (2001) 1123–1131.

Effects of α_1-Acid Glycoprotein on Erythrocyte Deformability and Membrane Stabilization

Kazuaki MATSUMOTO,[a] Katsuhide NISHI,[b] Yoshiko TOKUTOMI,[b] Tetsumi IRIE,[a] Ayaka SUENAGA,[a] and Masaki OTAGIRI*,[a]

[a] *Faculty of Pharmaceutical Sciences, Kumamoto University; 5–1 Oe-honmachi, Kumamoto 862–0973, Japan: and* [b] *School of Medicine, Kumamoto University; 2–2–1 Honjo, Kumamoto 860–0811, Japan.*
Received July 12, 2002; accepted September 24, 2002

The effects of α_1-acid glycoprotein (AGP) on human erythrocyte membrane were examined *in vitro*. Bovine and dog AGP, in addition to human AGP or asialo human AGP were used, and the collected data were compared with that for human serum albumin (HSA). A new technique developed by Kikuchi was used to investigate erythrocyte deformability. The addition of AGPs including human AGP facilitated the passage of human erythrocytes with an average diameter of 7.2 μm suspended in phosphate buffered saline (PBS) through a 5 μm wide microchannel; hemolysis was suppressed after the passage. The stabilizing effects of AGPs on membrane were evaluated. Human AGP prevented hemolysis induced by hypotonic phosphate buffer solution. The effects of human AGP on the oxidative changes in erythrocytes exposed to oxygen radicals were investigated. Human AGP protected erythrocytes from H_2O_2 and prevented the oxidation of dihydrorhodamine 123 to rhodamine 123 from H_2O_2. We propose that the antioxidant activity of human AGP is due to the binding of free radicals. In all studies, the effects of human AGP on erythrocytes might not be a function of the negative charge associated with sialyl residues, because the presence of *N*-acetylneuraminic acid had no effect. However, human AGP may promote microcirculation and antioxidant activity compared with HSA. No species differences in the physiological function of AGP were found. These results suggest that an increase in the AGP content of serum above the normal value found under pathological conditions facilitates the passage of erythrocytes through capillaries, stabilizes erythrocyte membranes and protects against oxidative stress, all of which are favorable for microcirculation.

Key words α_1-acid glycoprotein; erythrocyte deformability; antioxidant activity; erythrocyte osmotic fragility

Human α_1-acid glycoprotein (AGP) is a negatively charged acidic glycoprotein (pK_a=2.6; isoelectric point=2.7[1]), comprised of 59% protein and 41% carbohydrate[2]; it contains 11% sialic acid.[3] Human AGP, a normal serum constituent (75—100 mg/dl), with a molecular weight of approximately 44100, has been reported to be an acute phase reactant with increased plasma concentration in cases of pregnancy and inflammation and in cancer and other diseases.[4] AGP has also been reported to inhibit platelet aggregation,[5] to suppress proliferative response in lymphocyte cultures induced by anti-CD3[6] and phytohemagglutinin[7] and to increase the secretion of an IL-1 inhibitor by murine macrophages, most likely the IL-1 receptor antagonist.[8,9] However, its biological function is not yet fully understood. Maeda *et al.* previously reported that the addition of a small amount of AGP to a human erythrocyte suspension facilitated the passage of erythrocytes through artificial membrane filters with micropores having an average diameter smaller than that of an erythrocyte, and they proposed a possible physiological role for AGP in the microcirculation.[10]

The above findings prompted us to characterize the action of AGP on the membrane surface of erythrocytes. Thus, the present study was undertaken to investigate in detail the effects of AGP on erythrocyte membranes. Erythrocyte deformability was measured using a new technique developed by Kikuchi *et al.*[11] We also performed an osmotic fragility test with and without AGP. The capacity of erythrocytes to resist hemolysis can be characterized as the osmotic fragility of the membrane; osmotic fragility is classically used as a general screening procedure. We also investigated the effects of AGP on the oxidative changes in erythrocytes exposed to oxygen radicals, because AGP has been reported to inhibit neutrophil aggregation and superoxide anion generation induced by formyl-methionyl-leucyl-phenylalanine, phorbol myristate acetate[12] and phytohemagglutinin.[13] These studies were carried out using AGP and desialylated AGP to determine the role of sialic acid in this process.

MATERIALS AND METHODS

Materials Human, bovine and dog AGP (purified from Cohn fraction VI), human serum albumin (HSA), human γ-globulin, neuraminidase and dihydrorhodamine 123 (DRD) were obtained from Sigma Chemical Co. (St Louis, MO, U.S.A.). *N*-Acetylneuraminic acid was obtained from Nacalai Tesque (Kyoto, Japan). H_2O_2 was obtained from Santoku Chemicals Co. (Tokyo, Japan). All other materials were of reagent grade, and all solutions were prepared using deionized, distilled water.

Desialylation of AGP Human AGP was desialylated enzymatically, using methodology described by Primozic and McNamara,[14] using an immobilized neuraminidase obtained from *Clostridium perfringens*. Human AGP (40 mg) was dissolved in 5 ml of 67 mM phosphate buffer (pH 7.4) and 2 units of enzyme was added. The mixed solution was incubated at 37 °C, with gentle stirring at 60 rpm for 24 h. After incubation, the mixture was centrifuged and filtered to remove the immobilized enzyme. A small part of the filtrate was used for measuring sialic acid by the thiobarbituric acid method.[15] The product was dialyzed against deionized water and the dialysate lyophilized. Approximately 95% of sialic acid was removed, leaving an average of one sialic acid residue per protein molecule. The mol. Wt of asialo-AGP was therefore 40000.

* To whom correspondence should be addressed. e-mail: otagirim@gpo.kumamoto-u.ac.jp

Preparation of Erythrocyte Suspension Venous blood from the anticubital veins of healthy volunteers was collected in disposable syringes with a 21-gauge needle. After centrifugation at 3000 rpm for 10 min, the plasma and buffy coat were removed and replaced with phosphate buffered saline (PBS) (pH 7.4), and subsequently washed two times with PBS by repeated resuspension and centrifugation at 1000 rpm for 10 min. A 50% erythrocyte suspension was prepared in PBS.

Erythrocyte Deformability AGP, dissolved in PBS, was added to the washed erythrocytes, which were incubated for 3 h at 37 °C. Erythrocyte deformability was determined by Kikuchi's microchannel method.[11] The time required for 100 μl of erythrocytes to pass through a microchannel (MC-FAN; Hitachi Haramachi Electronics Co., Ltd.; width, 5 μm; length, 30 μm) was determined at a pressure of 20 cm H_2O. After filtration the erythrocytes were centrifuged at 3000 rpm for 3 min, and spectrophotometric measurements were then made on the supernatant at 540 nm to quantify the degree of hemolysis.

Osmotic Fragility Test Erythrocyte osmotic fragility was measured using washed erythrocytes, after 30 min incubation of the erythrocytes at 37 °C in solutions of 1.0—8.0 g/l phosphate buffered NaCl with and without AGP. The erythrocytes were centrifuged at 3000 rpm for 3 min, and spectrophotometric measurement of the supernatant was then made at 540 nm to quantify the degree of hemolysis.

Effects of AGP on Exposure of Erythrocytes to Oxygen Radicals A stock solution of 25 mM H_2O_2 was added to washed erythrocytes with and without AGP, and the resulting suspension incubated at 37 °C for 3 h in a shaking water bath. The erythrocytes were centrifuged at 3000 rpm for 3 min and the absorption of the supernatant at 540 nm was used to quantify the degree of hemolysis.

Reactive Oxygen Species (ROS) Quenching Capacity H_2O_2 oxidizes DRD to rhodamine 123 (RD), which fluoresces at 536 nm when excited at 500 nm. Two milliliters samples of AGP (45 μM) and DRD (5 μM) were prepared in 67 mM phosphate buffer, and at a predetermined time H_2O_2 (25 mM) was added. The progress of the reactions was followed spectrophotometrically by a fluorescence measurement of the RD formed. Controls were performed without any additives. Quenching of control was 0%.

Statistics Where possible, statistical analyses were performed by the Student's *t*-test.

RESULTS

Effects of AGP on Erythrocyte Passage throgh Microchannel Effects of bovine and dog AGP in addition to human AGP, HSA and *N*-acetylneuraminic acid on erythrocyte deformability are shown in Fig. 1. When the concentration of human AGP added to erythrocyte suspensions was increased, the passage time of erythrocytes through microchannels with an average diameter of 5 μm decreased. The effects of bovine, dog and asialo-human AGPs on the passage times were similar to those for human AGP; however, *N*-acetylneuraminic acid had no effect. This suggests that the enhancement was not a function of a negative charge related to the sialyl residues. The passage times for other serum proteins, HSA and γ-globulin were slightly but significantly slower

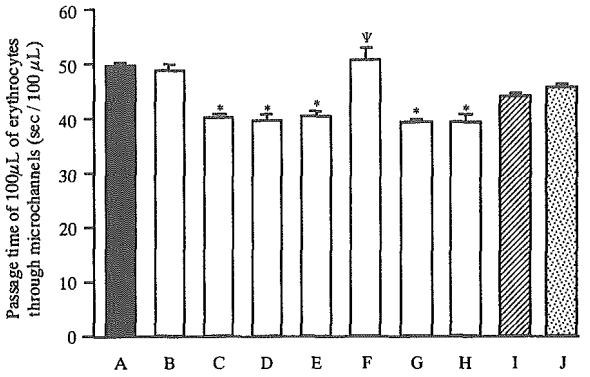

Fig. 1. Effects of AGPs on the Time Required for 100 μl Erythrocytes to Pass through Microchannels

11 μM and 23 μM AGP (normal concentration level). 45 μM AGP (above normal concentration level). A, without serum protein; B, 11 μM human AGP; C, 23 μM human AGP; D, 45 μM human AGP; E, 45 μM human asialo-AGP; F, 900 μM *N*-acetylneuraminic acid; G, 45 μM dog AGP; H, 45 μM bovine AGP; I, 45 μM HSA; J, 45 μM γ-globulin. The data are average values of 3—4 experiments (±S.D.). $*p<0.01$ as compared with HSA. $^{\Psi}p<0.005$ as compared with HSA.

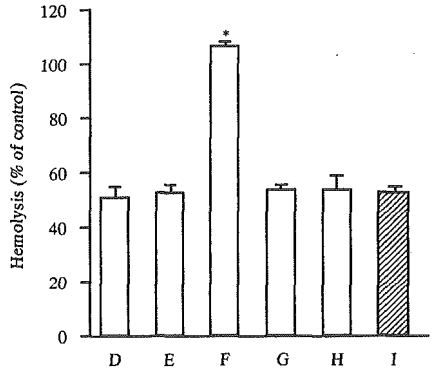

Fig. 2. Effects of AGPs on the Hemolysis of Erythrocytes during Passage through Microchannels

D, E, F, G, H and I are the same as shown in Fig. 1. The data are average values of 3—4 experiments (±S.D.). $*p<0.01$ as compared with HSA.

than those for AGPs, whereas the degree of hemolysis after passage was suppressed by nearly the same amount by AGPs and HSA, except for *N*-acetylneuraminic acid (Fig. 2).

Effects of AGP on Osmotic Fragility of the Erythrocyte Membrane To determine whether AGP contributes to the membrane stability or not, we performed an osmotic fragility test. Human AGP suppressed hemolysis induced by hypotonic phosphate buffer solution, and significant suppression was observed at 74 and 89 mOsm (data not shown). The suppressive effects of different AGPs, HSA and *N*-acetylneuraminic acid on hemolysis were determined at 74 and 89 mOsm. Effects of HSA, bovine, dog and asialo-human AGPs on hemolysis were similar to those of human AGP; however, *N*-acetylneuraminic acid had no effect (Table 1).

Antioxidant Activity of AGP to Erythrocytes Erythrocytes exposed to 25 mM H_2O_2 begin to undergo hemolysis after 1 h, and this increased gradually up to 3 h. The addition of different AGPs suppressed the hemolysis (Fig. 3). Table 2 shows the quenching capacities of human AGP and asialo-human AGP on DRD oxidation by H_2O_2. Both AGPs abolished the oxidation by H_2O_2 significantly. Interestingly, the antioxidant activities observed for AGPs were significantly higher than those of HSA (Fig. 3, Table 2).

Table 1. Effects of AGPs on Hemolysis at 74 mOsm

	Hemolysis (% of control)
23 μM Human AGP	84.4±1.7
45 μM Human AGP	82.6±2.9
45 μM Human asialo-AGP	82.3±3.1
900 μM *N*-Acetylneuraminic acid	104.5±4.3*
45 μM Dog AGP	84.0±1.5
45 μM Bovine AGP	82.6±2.5
45 μM HSA	82.8±3.3

The data are average values of 3—4 experiments (±S.D.). *$p<0.01$ as compared with HSA.

Table 2. Quenching of H_2O_2 Oxidation of DRD by Human AGP and HSA

	Quenching (%)
45 μM Human AGP	96.6±4.2*
45 μM Human asialo-AGP	92.7±3.8*
900 μM *N*-Acetylneuraminic acid	0.5±5.3#
45 μM HSA	70.2±11.7

The data are average values of three experiments (±S.D.). *$p<0.01$ as compared with HSA. #$p<0.001$ as compared with HSA.

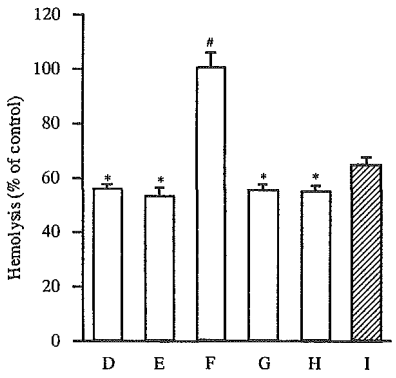

Fig. 3. Effects of AGPs on Hemolysis of Erythrocytes Induced by H_2O_2

D, E, F, G, H and I are the same as shown in Fig. 1. The data are average values of 3—4 experiments (±S.D.). *$p<0.01$ as compared with HSA. #$p<0.001$ as compared with HSA.

DISCUSSION

Our results show that the passage of human erythrocytes suspended in PBS through a microchannel 5 μm wide was facilitated and that hemolysis was suppressed by various AGPs (Figs. 1, 2). Although the reason AGP exhibited significant effects among the three serum proteins tested is not known, the effects for AGP might be due to the structural properties with five carbohydrate chains, different from HSA and γ-globulin. However, it should be noted that *N*-acetylneuraminic acid, a component of AGP, has no effect on the membrane. We know the effects on passage and hemolysis are not a function of negative charge on the sialyl residues (Figs. 1, 2). The issue of how AGP affects erythrocyte deformability is not fully understood. Maeda *et al.* previously showed that human AGP is bound to the surface of the erythrocytes as evidenced by fluorescent antibody staining.[10] They suggest that human AGP added to the suspension forms a lubricating film on the surface of erythrocytes by binding to the surface, thus reducing the friction between the erythrocytes and the microchannel.

They also showed that human AGP is able to stabilize the membrane by binding to the surface of the erythrocytes. In fact, human AGP prevented hemolysis induced by hypotonic phosphate buffer solution (Table 1), but the sialic acid may not play a role in this effect (Table 1).

The present studies show that human AGP, at physiological concentrations, protects erythrocytes from H_2O_2 (Fig. 3). Pukhal'skii *et al.* reported that human AGP inhibits neutrophil superoxide anion generation and suggested that the antioxidant activity of AGP is due to the binding of free radicals, rather than to the inhibition of neutrophil activation.[13] The data obtained here support this proposal. Based on this mechanism, it is possible that AGP prevents the oxidation of DRD to RD from H_2O_2 (Table 2).

It has been reported that bovine AGP inhibits ischemia/reperfusion injury by preventing apoptosis and inflammation[16] and prevents Gram-negative infections.[17] Since AGP is highly homologous among the species,[18,19] it seems reasonable that there are species differences in the physiological function of AGP which have not been found (Figs. 1—3, Table 1).

We propose that an increase in the AGP content of the serum above the normal value found under pathological conditions[4] facilitates the passage of erythrocytes through capillaries, stabilizes erythrocyte membranes and protects against oxidative stress, which would be a favorable situation for microcirculation. In fact, under pathological conditions of highly elevated fibrinolytic or clotting activity, antigen–antibody complex formation and oxidative stress takes place which impedes blood circulation in the capillaries. However, an elevation in AGP levels in the plasma should facilitate the microvascular passage of erythrocytes and stabilize the membrane. These limited data indicate that AGP may function as an important factor in homeostatic mechanisms that operate during microcirculation, although a molecular mechanism for the function of AGP remains to be elucidated.

REFERENCES

1) Schmid K., "The Plasma Proteins, Structure, Function and Genetic Control," 2nd ed., Vol. 1, ed. by Putnam F. W., Academic Press, New York, 1975, pp. 183—228.
2) Hao Y. L., Wickerhauser M., *Biochim. Biophys. Acta*, **322**, 99—108 (1973).
3) Schmid K., *Prog. Clin. Biol. Res.*, **300**, 7—22 (1989).
4) Israili Z. H., Dayton P. G., *Drug Metab. Rev.*, **33**, 161—235 (2001).
5) Snyder S., Coodley E. L., *Arch. Intern. Med.*, **136**, 778—781 (1976).
6) Pos O., Oostendorp R. A., van der Stelt M. E., Scheper R. J., Van Dijk W., *Inflammation*, **14**, 133—141 (1990).
7) Pukhal'skii A. L., Toptygina A. P., Kalashnikova E. A., Shiian S. D., Nasonov V. V., Bovin N. V., Liutov A. G., Bairushin F. T., *Biull. Eksp. Biol. Med.*, **118**, 71—73 (1994).
8) Bories P. N., Feger J., Benbernou N., Rouzeau J. D., Agneray J., Durand G., *Inflammation*, **14**, 315—323 (1990).
9) Tilg H., Vannier E., Vachino G., Dinarello C. A., Mier J. W., *J. Exp. Med.*, **178**, 1629—1636 (1993).
10) Maeda H., Morinaga T., Mori I., Nishi K., *Cell. Struct. Funct.*, **9**, 279—290 (1984).
11) Kikuchi Y., Sato K., Mizuguchi Y., *Microvasc. Res.*, **47**, 126—139 (1994).
12) Costello M. J., Gewurz H., Siegel J. N., *Clin. Exp. Immunol.*, **55**, 465—472 (1984).
13) Pukhal'skii A. L., Shmarina G. V., Kalashnikova E. A., Shiyan S. D., Kokarovtseva S. N., Pukhal'skaya D. A., Bovin N. V., *Bull. Exp. Biol.*

Med., **129**, 480—483 (2000).
14) Primozic S., McNamara P. J., *J. Pharm. Sci.*, **74**, 473—475 (1985).
15) Warren L., *J. Biol. Chem.*, **234**, 1971—1975 (1959).
16) Daemen M. A., Heemskerk V. H., van't Veer C., Denecker G., Wolfs T. G., Vandenabeele P., Buurman W. A., *Circulation*, **102**, 1420—1426 (2000).
17) Hochepied T., Van Molle W., Berger F. G., Baumann H., Libert C., *J. Biol. Chem.*, **275**, 14903—14909 (2000).
18) Ricca G. A., Taylor J. M., *J. Biol. Chem.*, **256**, 11199—11202 (1981).
19) Ray B. K., Ray A., *Biochem. Biophys. Res. Commun.*, **178**, 507—513 (1991).

総　説

α_1-酸性糖蛋白質の血液循環系に及ぼす作用

Effects of α_1-acid glycoprotein on blood circulation

松元一明[a]，岡本茂洋[a]，徳冨芳子[b]，徳冨直史[b]，西勝英[b]，丸山徹[a]，末永綾香[a]，小田切優樹[a]

Kazuaki Matsumoto[a], Shigehiro Okamoto[a], Yoshiko Tokutomi[b], Naofumi Tokutomi[b], Katsuhide Nishi[b], Toru Maruyama[a], Ayaka Suenaga[a], Masaki Otagiri[a]

和文抄録

急性期反応物質であるα_1-酸性糖蛋白質（AGP）は主に肝臓で合成され、炎症、火傷などでは血液中濃度は数倍増加することが知られている。しかしながら、AGPの生理作用についてはまだ十分に明らかにされていない。そこで、AGPの血液循環動態や生理作用の機序解明の基礎的検討の一環として、AGPの体内動態特性ならびに赤血球及び血管に対するAGPの影響について検討した。その結果、AGPは赤血球の流れを促進し、血管を弛緩させ、血液循環をより良いものにすることで、火傷時などの末梢循環系における組織の低酸素血症の防止に極めて重要な働きをしていることが推察された。

Abstract

α_1-Acid glycoprotein (AGP) is an acute phase protein that is synthesized largely by the liver. AGP serum concentrations that remain stable under physiological conditions (about 0.5 - 1.0 g/L) increase several-fold during inflammation or burn. However, its exact biological function and mechanism of action remain obscure.

In this review, we report pharmacokinetics and pharmacodynamics of AGP in elucidating of action of AGP. An increase in the AGP content of serum found under pathological conditions may improve blood rheology based upon its own activity. These findings will be useful in terms of understanding the role of acute phase proteins that are produced of an accelerated rate during acute phase response.

Keywords

α_1-acid glycoprotein, blood rheology, pharmacokinetics, biological function, blood cell

1．はじめに

ヒトα_1-酸性糖蛋白質（AGP）は、分子量約44100で、183個のアミノ酸と5本のN-結合型糖鎖からなり、その糖鎖末端にはシアル酸が結合している[1-4]。したがって、約40%の高い糖含量と低いpI値2.7を特徴とする血漿蛋白質である。またその糖鎖のN-アセチルグルコサミンにフコースが結合したシアリルルイスX（sLe^X）型を形成する場合もある。通常、健常人のAGP1分子当たり約60%がフコシル化されている[5]。

AGPはイヌの摘出肝実験[6]やラット肝臓の灌流実験[7]により、肝臓での生合成が明らかにされ、血中のAGPの大部分は肝臓で作

a 熊本大学大学院薬学教育部薬物動態制御学分野　〒862-0973　熊本市大江本町5-1

b 熊本大学大学院医学教育部生体機能薬理学分野　〒860-8556　熊本市本荘1-1-1

a Department of Biopharmaceutics, Graduate School of Pharmaceutical Sciences, Kumamoto University; 5-1 Oe-honmachi, Kumamoto 862-0973, Japan

b Department of Cell and Biological Pharmacology, Graduate School of Medical Sciences, Kumamoto University; 1-1-1 Honjo, Kumamoto 860-8556, Japan.

小田切　優樹

熊本大学大学院薬学教育部薬物動態制御学分野　〒862-0973　熊本市大江本町5-1

Department of Biopharmaceutics, Graduate School of Pharmaceutical Sciences, Kumamoto University; 5-1 Oe-honmachi, Kumamoto 862-0973, Japan

論文受付　2003年6月2日　　受理　2003年6月19日

られると考えられている。Weisman[8]らは^{131}I-AGPのturn overから、その半減期を5日と報告している。また、その血漿中濃度は、健常時に0.5～1.0 g/Lであるが[9]、炎症、火傷、感染症、腫瘍（癌）、心筋梗塞、妊娠時などに血液及び組織中で2～4倍増加する[10,11]。このAGPの誘導・発現は、免疫、炎症反応に重要なインターロイキン1（IL-1）、インターロイキン6、腫瘍壊死因子α（TNF-α）といった炎症性サイトカイン及び糖質コルチコイドにより制御されていることが報告されている[12,13]。興味深いことに、Table 1に示すように、AGPは肝臓だけでなく炎症反応に深く関わりのある単球、リンパ球、血管内皮細胞などでも合成され[14]、さらに、炎症部位に局在することが蛍光電顕などで明らかにされている[15,16]。そのため従来より生合成が亢進する急性炎症時に、AGPはその病巣部位で何らかの働きをしているものと推察されてきた。現在までに報告されているAGPの生理作用としては、例えば、血小板凝集抑制[17,18]、IL-1レセプターアンタゴニスト誘導[19,20]、リンパ球増殖抑制[21,22]、抗好中球活性、抗補体活性[23]などがある。また、最近では白血球と血管内皮細胞の接着因子であるセレクチンと高親和性のsLe^{x}残基の発現増大が炎症時AGPで観察されており[24]、セレクチンとsLe^{x}残基の結合をAGPが阻害する可能性も見出されている[25]。さらに、AGPは微小血管の内皮細胞に結合し、自身の負電荷を供与することにより[26,27]、ポリアニオン高分子量蛋白質の血管透過抑制に関与していると考えられている[26,28]。このように、AGPの抗炎症効果や免疫抑制効果については数多くの報告がなされている。しかしながら、急性炎症は、局所における微小循環系を中心としたものである。急性炎症時には、腫瘍壊死因子などのサイトカインによりもたらされる活性酸素などによって赤血球膜障害が起こり、異型化した赤血球がマクロファージによる貪食反応を受けるようになる。

なかでも脾臓は特有のフィルター構造が発達しており、停滞した赤血球に対し代謝的ストレスを与えることと相まって、変形能の低下した赤血球を高感度に検出して除去し、貧血や組織の低酸素血症を引き起こすことが知られている[29,30]。また火傷時では、大量の体液が失われ、浸透圧低下や末梢循環血流量が減少する結果、末梢組織への酸素供給が不足し、ショック症状を引き起こす。また、組織の修復過程における細胞の増殖と分化、さらに損傷部位の再形成にとって損傷組織への血液供給は極めて重要である。

そこで本稿では、AGPの血液循環系への作用について、最近、当研究室で得られた知見を中心に紹介する。

Table 1 Extra-hepatic expression of AGP

Organs or cell types	Protein	mRNA	Constitutive	Inducible
Kidney		+	−	+
Adipose		−		
Spleen		−		
Thymus		−		
Heart	+	−	+	
Testis		−		
Ileum	+			+
Stomach	+			+
Colon	+		+	+
Intestinal epithelial cell		+		+
Prostatic epithelial cell	+			+
Brain		−		
Breast	+		+	+
Breast epithelial cell	+		+	
Uterus			−	
Decidua	+			+
Lung	+	−+	−	+
Pulmonary fibroblast		+		+
Pneumocyte II	+	+	−	+
Alveolar macrophage	+	+	−+	+
Peritoneal macrophage		−		
Monocyte	+		+	+
Lymphocyte	+		+	+
Granulocyte	+		+	+
Endothelial cell	+	+	+	

The expression (+) or the absence of expression (-) of AGP protein and mRNA are described for the extra-hepatic tissues and cell types studied. When the AGP gene expressed, constitutive (basal) or inducible (inflammation, cancer) expression in the corresponding tissue or cell type is indicated.
Fournier et al., *Biochim. Biophys. Acta*, **1482**: 157-171 (2000)

2．AGPの体内動態特性

作用部位などを考える場合、AGPやその糖修飾体の生体内における動態を明らかにすることは、AGPの構造・機能発現という観点から大変興味深い。一般にAGP、セルロプラスミン、フェツインなどの糖蛋白質の半減期は数時間であるのに対し、糖鎖末端のシアル酸をシアリダーゼにより除去し、アシアロ体にすると半減期は数分になる。これはシアル酸を除去することにより、Fig. 1に示すように、露出したガラクトースが肝臓のアシアログリコプロテインレセプターに認識され、取り込まれることによって生じることが明らかにされている[31,32]。この仮説を実証すべく、石橋らはアシアログリコプロテインレセプターノックアウトマウスを作成し、AGPの血中濃度推移をノーマルマウスと比較検討したところ、予想に反し両者共にまったく同様な血中濃度推移を示した。このことから、著者らはAGPの血中からの消失にはアシアログリコプロテインレセプター以外の経路が関与している可能性を報告している[33]。このように、AGPの消失経路や消失部位については、様々な説があり、未だ不明瞭な点が多く残されている。しかしながら、生体内において様々な生理作用を発揮するのは未変化体のAGPであると考えられる。なぜなら、生体内で糖蛋白質がシアリダーゼによりアシアロ体になるという報告は未だなく（Fig. 1）、仮に、生体内でAGPがアシアロAGPになったとしてもすぐに肝臓のアシアログリコプロテインレセプターに取り込まれることは明らかで[31]、生体内には未変化体のAGPしか存在していないと考えられる。

また当研究室で^{131}I標識したAGPをマウス尾静脈より投与し、30分後における臓器分布を調べた結果、AGPはほとんど消失部位である肝臓と血液中に存在した。さらに、血液中に存在するAGPのうち約3分の1は血球中に存在することが示唆され、

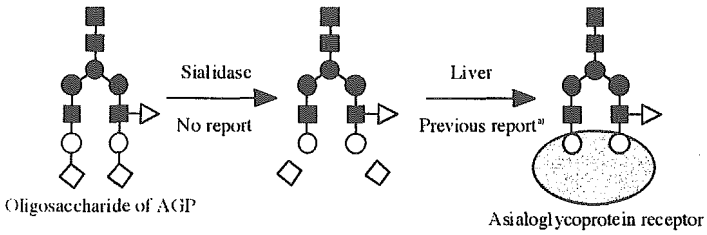

Fig. 1 A model for elimination route of AGP
Terminal sialic acid residues were removed by sialidase, then desialylated (terminal galactose residues) AGP was uptaked in asialoglycoprotein receptor on parenchymal cells of the liver.
■ : N-acetylglucosamine, ● : mannose, ○ : galactose,
◇ : sialic acid, ▷ : fucose.
a); Morell A. G., et al., *J. Biol. Chem.*, **246**: 1461-7 (1971)

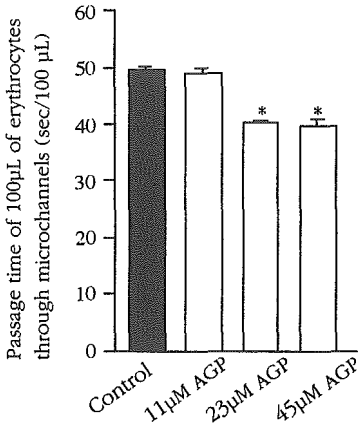

Fig. 2 Effects of AGP on the time required for 100 μL erythrocytes to pass through microchannels
The data are average values of 3 - 4 experiments (±S. D.).
*P < 0.01 as compared with control.

AGPが血管及び血球に対して何らかの影響を及ぼしている可能性が十分に考えられた。

3．赤血球に対するAGPの影響

両凹円盤状の特徴的な形状を持つ赤血球の径はヒトの場合約7.2～8μmあり、毛細血管の平均的径（5～6μm）より大きい。したがって、赤血球は変形して毛細血管を通過することになる。そのため、赤血球の変形能が毛細血管での血流速度ないし血流量を左右する最も重要な因子になる。一方、赤血球の主な役割は酸素運搬であるが、そのためには正常な細胞形態と機能が不可欠である。特に末梢循環系における赤血球の変形能は、組織の低酸素血症の防止に極めて重要な働きをしている。そこでまず、菊池らによって開発された半導体微細加工技術（集積回路制作技術）を用いてシリコン単結晶基板表面に加工した微細な溝（マイクロチャンネル）のアレイを毛細血管モデルとして用いる流動性測定法により[34]、AGPの赤血球変形能に対する影響を調べた。すなわち、等張リン酸緩衝液に50%に調製した健常人の赤血球がポアサイズ5μmのマイクロチャンネルを100μL通過するために要する時間を測定した。Fig. 2に示すように、AGPは健常人の血中濃度である23μM、炎症時の血中濃度である45μMにおいて、赤血球のマイクロチャンネル通過時間を有意に短縮した。さらに、マイクロチャンネル通過後の赤血球の溶血の度合いを調べたところ、AGPは通過後の溶血を有意に抑制した。したがって、AGPは赤血球の変形能を良好にし、毛細血管における赤血球の流れを改善することが示唆された。

赤血球を低張の塩化ナトリウムを含むリン酸緩衝液（pH 7.4）に浮遊させると、赤血球内は外部より高張であるので、水分は血球内に入り込み、結果として膨張し球状となり、遂には膜が破れて溶血に至る。この原理を利用して赤血球膜の安定性を評価した[35]。50%に調製した赤血球は約150mOsm以下で有意な溶血が認められたが、その溶血を23、45μMのAGPは有意に抑制した。このとき用いたAGPによる浸透圧の変化は認められなかった。したがって、AGPには赤血球膜安定化作用があることが示唆された。

急性炎症時には、腫瘍壊死因子などのサイトカインによりもたらされる活性酸素などによって赤血球膜障害が起こり、異型化した赤血球がマクロファージによる貪食を受けたり、脾臓のフィルターにより変形能の低下した赤血球が検出され除去されたりする[29]。そこで、AGPが活性酸素種添加による赤血球膜障害を抑制するかどうか検討した。25mMのH_2O_2を50%に調製した赤血球に添加すると、1時間で膜障害による溶血が確認され、3時間後まで増大した。そこで、H_2O_2添加3時間後における溶血の度合いを検討したところ、23、45μM AGPは有意に溶血を抑制した。次にジヒドロローダミン123がローダミン123に酸化されると蛍光を発する特徴を利用し[36]、25mMのH_2O_2による酸化をAGPが抑制するかどうか検討した。23、45μMAGPはH_2O_2添加によるローダミン123の蛍光を有意に抑制し、AGPには抗酸化活性があることを示した。また、AGPの糖鎖末端にあるシアル酸にはこのような作用はなく、アシアロAGPはAGPと同様な抗酸化活性を有していたことから、アルブミンと同様、赤血球の代わりにAGPのペプチド部分が活性酸素種によって酸化され、赤血球を活性酸素種から守っているのかもしれない。

以前、AGPが赤血球膜表面に結合していることが報告されている[37]。すなわち、AGPは赤血球膜表面に結合することによって、毛細血管を通過するときは潤滑油の役目をし、さらに膜を安定化させ、AGP自ら酸化されることで外敵から赤血球を守っている可能性が示唆された。

4．血管に対するAGPの影響

前項において、AGPによる組織修復効果のメカニズムの可能性として、循環改善、すなわち血流促進作用を作業仮説とし、AGPが赤血球の流動性を改善していることを示唆した。次に、マウス胸部大動脈摘出標本にAGPを直接作用させて弛緩反応が得られるかどうかについて、等尺性張力測定法（Magnus法）[38]を用いて検討した。2本のワイヤーで標本が垂直になるように留め、95%O_2-5%CO_2で十分に通気し、37℃に温めた栄養液で

満たした標本層中で実験を行った。α_1受容体アゴニストであるフェニレフリンのα_1受容体刺激で活性化されたホスホリパーゼCによりイノシトール3-リン酸が生成され、そのイノシトール3-リン酸により細胞内カルシウム貯蔵部位からカルシウムが放出されて、カルシウム濃度が上昇し、血管の収縮が起こる[39]。Fig. 3に示すように、標本に対してフェニレフリン（0.1 μM）前処理により立ち上がりの速い収縮が現れ、その後、その収縮は持続した。また、フェニレフリンによる収縮が見られた後、AGPを投与すると濃度依存的に弛緩した。これらのことから、AGPは血管弛緩作用を有することが示唆された。

血管においては、内皮細胞由来弛緩因子、すなわちNOが平滑筋弛緩作用を示す。その弛緩のメカニズムは、まず内皮細胞において様々な生理活性物質やアゴニストの受容体が活性化されて起こるカルシウム濃度上昇がきっかけとなっている。カルシウム濃度が上昇すると、活性型のカルシウム/カルモジュリン複合体が形成され、カルシウム/カルモジュリン依存性のNO合成酵素が活性化される。その結果、産生されるNOが平滑筋細胞内に移動し、そこでグアニレートシクラーゼを活性化させ、サイクリックグアノシン 3', 5'-1-リン酸（cGMP）量が増加し、cGMP依存性プロテインキナーゼが活性化される。このキナーゼによって、細胞膜のカリウムチャンネル及びホスホリパーゼC、筋小胞体のカルシウム放出チャンネル及びカルシウムポンプがリン酸化されることでカルシウム濃度が減少し、平滑筋の弛緩が生じる[40]。そこで、AGPの血管弛緩作用がNOを介して起こるかどうか検討するために、NO合成阻害剤であるN^G-nitro-L-arginine methyl ester（L-NAME）前処理後の標本に対するAGPの影響をみた。さらに、内皮細胞を除去した標本に対する影響も検討した。アセチルコリンはM1受容体を介してNO合成酵素を活性化し、血管を弛緩することが報告されている[41]。フェニレフリン誘導収縮をアセチルコリン（1 μM）は弛緩させたが、報告通りL-NAME（1mM）の前処理により弛緩の抑制が見られた。しかしながら、AGPの弛緩作用はL-NAMEにより抑制されなかった。他のNO合成阻害剤であるN^G-monomethyl-L-arginine（0.1mM）においてもアセチルコリンの弛緩作用は抑制されたが、AGPの弛緩作用は影響されなかった。これらのことから、AGPの弛緩作用にNOは関与しないことが示唆された。また、内皮細胞除去によりアセチルコリンの弛緩作用は抑制されたが、AGPの弛緩作用への影響は認められず、内皮細胞の寄与はないことが示唆された。したがって、AGPの弛緩作用に内皮細胞由来のNOの関与はなく、直接平滑筋細胞に作用することが示唆された。

ヘパリンはカルシウムに依存してセレクチンと結合し、sLe^X残基のセレクチンへの結合を阻害することが知られている[42, 43]。そこで、ヘパリンの前処理が、フェニレフリン誘導収縮に対するAGPの弛緩作用に影響を与えるかどうか検討した。その結果、ヘパリン（100unit/mL）はAGPの弛緩作用を抑制した。また、アセチルコリンの弛緩作用には影響を与えなかった。ヘパリンはsLe^X残基を含むリガンドとセレクチンの結合を特異的に阻害し、急性炎症時、腹腔内への好中球の流入を減少させることが

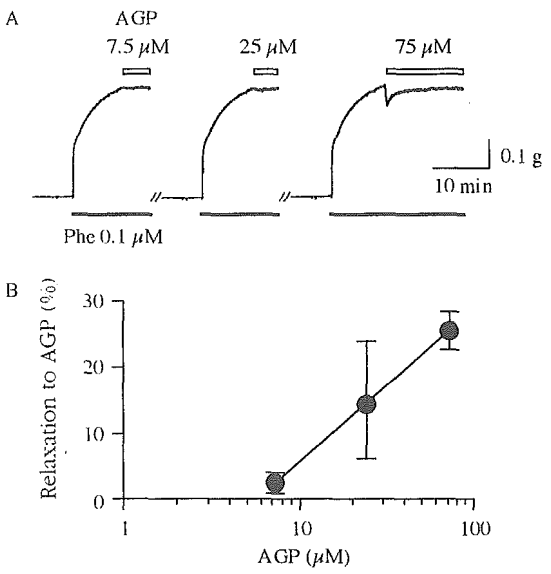

Fig. 3 Concentration-dependent relaxation with AGP
(A) Representative traces showing the AGP-induced relaxation at indicated concentrations in Phenylephrine (Phe) (0.1μM)-precontracted rings of mouse aorta. (B) Average concentration-relaxation curves to AGP from experiments as depicted in (A). The relaxations are expressed in per cent of the maximal Phe-induced contraction prior to application of AGP. The data are average values of 5 - 26 experiments (±S. D.).

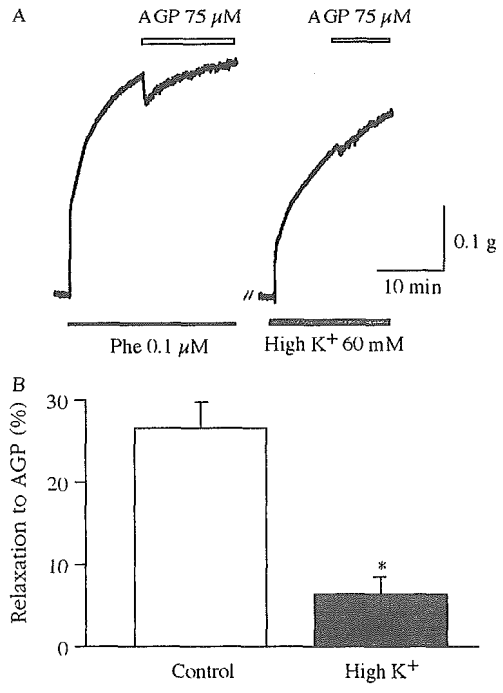

Fig. 4 Relaxations to AGP in aortic rings precontracted with K^+ solution
(A) Representative traces showing the AGP-induced relaxation in Phe (0.1 μM)- and high K^+ (60 mM)-precontracted aortic rings. (B) Average relaxation to AGP (75 μM) in the Phe-precontracted (open column) and high K^+-precontracted (dotted column) rings from experiments as depicted in (A). Values (mean±S.D.) are expressed as per cent reversal of the maximal Phe- induced contraction prior to application of AGP. *P < 0.01 vs. control.

報告されているので[42, 43]、今回の結果は、ヘパリンが平滑筋細胞表面に発現したレクチン様ドメインとAGPのsLe^{x}残基との結合を阻害したことにより惹起された可能性が考えられる。

AGPの弛緩作用が前処理の方法によって変わるかどうか検討するために、高濃度のカリウム溶液で前処理を行い、フェニレフリンによる前処理のときと比較した。Fig.4に示すように、栄養液中のカリウムを通常の5mMから60mMまで増やした高カリウム溶液の方が、フェニレフリンを前処理したときよりAGPの弛緩作用の程度は小さかった。なお、細胞外カリウム濃度を増やすと平滑筋細胞膜が脱分極し、電位依存性カルシウムチャンネルが活性化されて開き、カルシウムが細胞内へ流入するため、細胞内カルシウム濃度が上昇して収縮する[44]。すなわち、今回の結果からAGPの弛緩作用は電位依存性カルシウムチャンネルよりむしろα_1受容体の活性化による収縮反応に対して効果があることが示唆された。

最近、唐木らは平滑筋細胞でα_1受容体刺激による非選択的カチオンチャンネルが収縮に関与することを示し、平滑筋細胞のα_1受容体活性化がイノシトール3-リン酸依存性のカルシウム放出と非選択的カチオンチャンネルを介したカルシウム流入によって、細胞内カルシウム濃度を増加させることを報告した[45]。以上のことから、AGPの血管弛緩作用は、AGPが平滑筋細胞膜上のレクチン様ドメインに結合し、α_1受容体刺激によるイノシトール3-リン酸依存性のカルシウム放出、及び非選択的カチオンチャンネルを介したカルシウム流入の阻害によるものと、作用としては小さいものの、電位依存性のカルシウムチャンネルからのカルシウム流入を阻害することによって引き起こされることが示唆された（Scheme 1）。

5．おわりに

急性期蛋白質であるAGPは赤血球に対して変形能改善作用、膜安定化作用、抗酸化作用を有することが示唆された。さらに、AGPはマウス大動脈平滑筋細胞のレクチン様ドメインに結合し、血管拡張作用を示すことが示唆された。また、その作用機序として、イノシトール3-リン酸依存性のカルシウム放出阻害、及び非選択的カチオンチャンネルの阻害、作用としては小さいが電位依存性カルシウムチャンネルの阻害が示唆された。すなわち、AGPは生合成が亢進する急性炎症時に、赤血球の流れを保護し、血管を拡張させ、血液循環をより良いものにすることで、末梢循環系における組織の低酸素血症などの防止に極めて重要な働きをしていると推察される。

これらの知見は、急性期蛋白質AGPの生体内での役割の一端を明らかにしたもので、今後、医薬品開発上の観点から更なるデータの蓄積が望まれる。

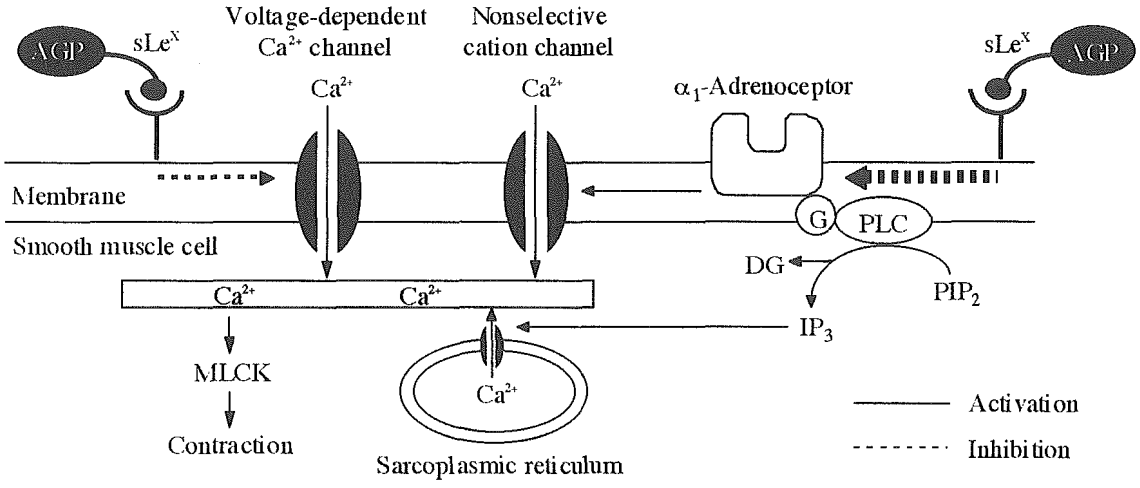

Scheme 1 Mechanism of vasorelaxant effect by AGP

G：G protein, PLC：phospholipase C, PIP_2：phosphatidylinositol-4, 5-bisphosphate, IP_3：inositol-1, 4, 5-trisphosphate, DG：1,2-diacylglycerol, MLCK：myosin light chain kinase, sLe^X：sialyl Lewis X.

Reference

1. Schmid K, Kaufmann H, Isemura S, Bauer F, Emura J, Motoyama T, Ishiguro M, Nanno S. Structure of alpha 1-acid glycoprotein. The complete amino acid sequence, multiple amino acid substitutions, and homology with the immunoglobulins. Biochemistry 1973;12:2711-24.
2. Schmid K, Burgi W, Collins JH, Nanno S. The disulfide bonds of alpha 1-acid glycoprotein. Biochemistry 1974;13:2694-7.
3. Aubert JP, Loucheux-Lefebvre MH. Conformational study of alpha 1-acid glycoprotein. Arch. Biochem. Biophys. 1976;175:400-9.
4. Schmid K, Binette JP, Dorland L, Vliegenthart JF, Fournet B, Montreuli J. The primary structure of the asialo-carbohydrate units of the first glycosylation site of human plasma alpha 1-acid glycoprotein. Biochim. Biophys. Acta 1979;581:356-9.
5. Van Dijk W, Poland DCW. Occurrence and anti-inflammatory properties of specific glycoforms of human alpha 1-acid glycoprotein. Proceedings of the International Symposium on Serum Albumin and Alpha 1-Acid Glycoprotein (Eds. M Otagiri, Y Sugiyama, B Testa, J-P Tillement), Tokyo Print, Kumamoto, Japan 2000;115-22.
6. Athineos E, Kukral JC, Winzler RJ. The site of glucosamine incorporation into canine plasma alpha 1-acid glycoprotein. Arch. Biochem. Biophys. 1964;106:338-42.
7. Sarcione EJ. Synthesis of alpha 1-acid glycoprotein by the isolated perfused rat liver. Arch. Biochem. Biophys. 1963;100:516-9.
8. Weisman S, Goldsmith B, Winzler R, Lepper MH. Turnover of plasma orosomucoid in man. J. Lab. Clin. Med. 1961;57:7-15.
9. Kremer JM, Wilting J, Janssen LH. Drug binding to human alpha 1-acid glycoprotein in health and disease. Pharmacol. Rev. 1988;40:1-47.
10. Kushner I. The phenomenon of the acute phase response. Ann. N. Y. Acad. Sci. 1982;389:39-48.
11. Fey GH, Fuller GM. Regulation of acute phase gene expression by inflammatory mediators. Mol. Biol. Med. 1987;4:323-38.
12. Baumann H, Firestone GL, Burgess TL, Gross KM, Vamamoto KR, Held WA. Dexamethasone regulation of alpha 1-acid glycoprotein and other acute phase reactants in rat liver and hepatoma cells. J. Biol. Chem. 1983;258:563-70.
13. Kulkarni AB, Reinke R, Feigelson P. Acute phase mediators and glucocorticoids elevate alpha 1-acid glycoprotein gene transcription. J. Biol .Chem. 1985;260:15386-9.
14. Fournier T, Medjoubi NN, Porquet D. Alpha 1-acid glycoprotein. Biochim. Biophys. Acta 2000;1482:157-71.
15. Shibata K, Okubo H, Ishibashi H, Tsuda-Kawamura K, Yanase T. Rat alpha 1-acid glycoprotein: uptake by inflammatory and tumour tissues. Br. J. Exp. Pathol. 1978;59:601-8.
16. Jamieson JC, Turchen B, Huebner E. Evidence for the presence of rat alpha 1-acid glycoprotein in granuloma tissue: a fluorescence microscopy study. Can. J. Zool. 1980;58:1513-7.
17. Snyder S, Coodley EL. Inhibition of platelet aggregation by alpha 1-acid glycoprotein. Arch. Intern. Med. 1976;136:778-81.
18. Costello M, Fiedel BA, Gewurz H. Inhibition of platelet aggregation by native and desialised alpha 1-acid glycoprotein. Nature 1979;281:677-8.
19. Bories PN, Feger J, Benbernou N, Rouzeau JD, Agneray J, Durand G. Prevalence of tri- and tetraantennary glycans of human alpha 1-acid glycoprotein in release of macrophage inhibitor of interleukin-1 activity. Inflammation 1990;14:315-23.
20. Tilg H, Vannier E, Vachino G, Dinarello CA, Mier JW. Antiinflammatory properties of hepatic acute phase proteins: preferential induction of interleukin 1 (IL-1) receptor antagonist over IL-1 beta synthesis by human peripheral blood mononuclear cells. J. Exp. Med. 1993;178:1629-36.
21. Pos O, Oostendorp RA, Van der Stelt ME, Scheper RJ, Van Dijk W. Con A-nonreactive human alpha 1-acid glycoprotein (AGP) is more effective in modulation of lymphocyte proliferation than Con A-reactive AGP serum variants. Inflammation 1990;14:133-41.
22. Pukhal'skii AL, Toptygina AP, Kalashnikova EA, Shiian SD, Nasonov VV, Bovin NV, Liutov AG, Bairushin FT. Immunomodulating effects of alpha 1-acid glycoprotein (orosomucoid) in cultured human peripheral blood lymphocytes. Biull. Eksp. Biol. Med. 1994;118:71-3.
23. Williams JP, Weiser MR, Pechet TT, Kobzik L, Moore FDJr, Hechtman HB. Alpha 1-acid glycoprotein reduces local and remote injuries after intestinal ischemia in the rat. Am. J. Physiol. 1997;273:G1031-5.
24. De Graaf TW, Van der Stelt ME, Anbergen MG, Van Dijk W. Inflammation-induced expression of sialyl Lewis X-containing glycan structures on alpha 1-acid glycoprotein (orosomucoid) in human sera. J. Exp. Med. 1993;177:657-66.
25. Jorgensen HG, Elliott MA, Priest R, Smith KD. Modulation of sialyl Lewis X dependent binding to E-selectin by glycoforms of alpha 1-acid glycoprotein expressed in

rheumatoid arthritis. Biomed. Chromatogr. 1998;12:343-9.
26. Curry FE, Rutledge JC, Lenz, JF. Modulation of microvessel wall charge by plasma glycoprotein orosomucoid. Am. J. Physiol. 1989;257:H1354-9.
27. Schnitzer JE, Pinney E. Quantitation of specific binding of orosomucoid to cultured microvascular endothelium: role in capillary permeability. Am. J. Physiol. 1992;263:H48-55.
28. Haraldsson B, Rippe B. Orosomucoid as one of the serum components contributing to normal capillary permselectivity in rat skeletal muscle. Acta Physiol. Scand. 1987;129:127-35.
29. Yoshida M, Kajii E, Kitagawa S. Macrophages and erythrocytes. Rinsho Ketsueki 1989;30:1244-7.
30. Shiga T, Maeda N. The aging and destruction of erythrocytes and rheology. Rinsho Ketsueki 1989;30:1256-60.
31. Morell AG, Gregoriadis G, Scheinberg IH, Hickman J, Ashwell G. The role of sialic acid in determining the survival of glycoproteins in the circulation. J. Biol. Chem. 1971;246:1461-7.
32. Morell AG, Irvine RA, Sternlieb I, Scheinberg IH, Ashwell G. Physical and chemical studies on ceruloplasmin. V. Metabolic studies on sialic acid-free ceruloplasmin in vivo. J. Biol. Chem. 1968;243:155-9.
33. Ishibashi S, Hammer RE, Herz J. Asialoglycoprotein receptor deficiency in mice lacking the minor receptor subunit. J. Biol. Chem. 1994;269:27803-6.
34. Kikuchi Y, Sato K, Mizuguchi Y. Modified cell-flow microchannels in a single-crystal silicon substrate and flow behavior of blood cells. Microvasc. Res. 1994;47:126-39.
35. Fujii H. Osmotic fragility test. Nippon Rinsho 1997;55 Suppl 1:153-5.
36. Hondal RJ, Motley AK, Hill KE, Burk RF. Failure of selenomethionine residues in albumin and immunoglobulin G to protect against peroxynitrite. Arch. Biochem. Biophys. 1999;371:29-34.
37. Maeda H, Morinaga T, Mori I, Nishi K. Further characterization of the effects of alpha 1-acid glycoprotein on the passage of human erythrocytes through micropores. Cell Struct. Funct. 1984;9:279-90.
38. Karaki H, Sato K, Ozaki H. Different effects of verapamil on cytosolic Ca2+ and contraction in norepinephrine-stimulated vascular smooth muscle. Jpn. J. Pharmacol. 1991;55:35-42.
39. Schnabel P, Nohr T, Nickenig G, Paul M, Bohm M. Alpha-adrenergic signal transduction in renin transgenic rats. Hypertension 1997;30:1356-61.
40. 平田結喜緒. NOのすべて. 東京：医歯薬出版, 1996;88-91.
41. Moncada S, Palmer RM, Higgs EA. Nitric oxide: physiology, pathophysiology, and pharmacology. Pharmacol. Rev. 1991;43:109-42.
42. Nelson RM, Cecconi O, Roberts WG, Aruffo A, Linhardt RJ, Bevilacqua MP. Heparin oligosaccharides bind L- and P-selectin and inhibit acute inflammation. Blood 1993;82:3253-8.
43. Koenig A, Norgard-Sumnicht K, Linhardt R, Varki A. Differential interactions of heparin and heparan sulfate glycosaminoglycans with the selectins. Implications for the use of unfractionated and low molecular weight heparins as therapeutic agents. J. Clin. Invest. 1998;101:877-89.
44. Imaizumi Y, Muraki K, Takeda M, Watanabe M. Measurement and simulation of noninactivating Ca current in smooth muscle cells. Am. J. Physiol. 1989;256:C880-5.
45. Karaki H, Ozaki H, Hori M, Mitsui-Siato M, Amano K, Harada K, Miyamoto S, Nakazawa H, Won KJ, Sato K. Calcium movements, distribution, and functions in smooth muscle. Pharmacol. Rev. 1997;49:157-230.

Am J Physiol Heart Circ Physiol 285: H1140–H1147, 2003.
First published May 8, 2003; 10.1152/ajpheart.00285.2003.

Improved oxygenation in ischemic hamster flap tissue is correlated with increasing hemodilution with Hb vesicles and their O_2 affinity

Claudio Contaldo,[1] Sören Schramm,[1] Reto Wettstein,[1] Hiromi Sakai,[2] Shinji Takeoka,[2] Eishun Tsuchida,[2] Michael Leunig,[1] Andrej Banic,[1] and Dominique Erni[1]
[1]*Department of Orthopedic, Plastic and Hand Surgery, Inselspital University Hospital, 3010 Berne, Switzerland; and* [2]*Advanced Research Institute for Science and Engineering, Waseda University, Tokyo 169-8555, Japan*

Submitted 1 April 2003; accepted in final form 5 May 2003

Contaldo, Claudio, Sören Schramm, Reto Wettstein, Hiromi Sakai, Shinji Takeoka, Eishun Tsuchida, Michael Leunig, Andrej Banic, and Dominique Erni. Improved oxygenation in ischemic hamster flap tissue is correlated with increasing hemodilution with Hb vesicles and their O_2 affinity. *Am J Physiol Heart Circ Physiol* 285: H1140–H1147, 2003. First published May 8, 2003; 10.1152/ajpheart.00285.2003.—The aim of this study was to test the influence of oxygen affinity of Hb vesicles (HbVs) and level of blood exchange on the oxygenation in collateralized, ischemic, and hypoxic hamster flap tissue during normovolemic hemodilution. Microhemodynamics were investigated with intravital microscopy. Tissue P_{O_2} was measured with Clark-type microprobes. HbVs with a P_{50} of 15 mmHg (HbV15) and 30 mmHg (HbV30) were suspended in 6% Dextran 70 (Dx70). The Hb concentration of the solutions was 7.5 g/dl. A stepwise replacement of 15%, 30%, and 50% of total blood volume was performed, which resulted in a gradual decrease in total Hb concentration. In the ischemic tissue, hemodilution led to an increase in microvascular blood flow to maximally 141–166% of baseline in all groups (median; $P < 0.01$ vs. baseline, not significant between groups). Oxygen tension was transiently raised to 121 ± 17% after the 30% blood exchange with Dx70 ($P < 0.05$), whereas it was increased after each step of hemodilution with HbV15-Dx70 and HbV30-Dx70, reaching 217 ± 67% ($P < 0.01$) and 164 ± 33% ($P < 0.01$ vs. baseline and other groups), respectively, after the 50% blood exchange. We conclude that despite a decrease in total Hb concentration, the oxygenation in the ischemic, hypoxic tissue could be improved with increasing blood exchange with HbV solutions. Furthermore, better oxygenation was obtained with the left-shifted HbVs.

blood substitutes; artificial red blood cells; microhemodynamics; hypoxia; collateral circulation

MAINTAINING ADEQUATE OXYGENATION is crucial for functional recovery and survival of cerebral, myocardial, mesenteric, or peripheral tissues rendered ischemic due to acute obstruction of their anatomic blood supply. In this scenario, oxygenation is determined by the amount of oxygen that is transported into the infarcted tissue via a collateral vasculature as well as by the potential of the oxygen carrier to deliver oxygen to this tissue.

Oxygenation and survival of ischemic myocardial (7, 19), cerebral (3, 18, 29), and peripheral tissues (2) could successfully be improved after the infusion of solutions containing artificial oxygen carriers, such as perfluorocarbons and chemically modified Hbs. These solutions have initially been developed with the scope of reducing the need of allogeneic blood transfusions, and at least four compounds are currently in advanced clinical trials to evaluate their potential as red blood cell (RBC) substitutes in blood loss (1, 10).

In a recent study (6), we were able to demonstrate that hypoxia in ischemic, collateralized hamster flap tissue was attenuated by a 50% blood exchange with a solution containing Hb vesicles (HbVs) suspended in 6% Dextran 70 (Dx70). The effect was associated with an increased capacity to transport oxygen to the ischemic tissue, which was related to the presence of HbVs and to an improvement of microcirculatory blood flow.

The HbV consists of isolated, purified human Hb that is encapsulated with a double phospholipid membrane coated with polyethylene glycol (22). The encapsulation of Hb prolongs the circulation time in the organism and prevents direct contact of Hb with the endothelial lining, thus suppressing vasoconstriction due to NO scavenging, which has been attributed to chemically modified Hbs (20). Another major advantage of the HbV is that oxygen affinity may easily be adapted to the needs of the tissue by supplementing the appropriate amount of coencapsulated allosteric effector (pyridoxal 5′-phosphate) (24). It was shown that after a 80% blood exchange with HbV solutions, oxygen consumption of the microvasculature was near to normal for a P_{50} of 16 and 30 mmHg, respectively, whereas it was significantly reduced for a P_{50} of 9 mmHg. The development of artificial RBC substitutes has been characterized by the assumption that their oxygen affinity should be similar or lower than that of blood to facilitate the delivery of oxygen to the tissues in need. On the other hand, it has been postulated that shifting the oxygen dissociation curve of RBC-bound Hb to the left (26, 27) or applying artificial oxygen

Address for reprint requests and other correspondence: D. Erni, Div. of Plastic and Reconstructive Surgery, Inselspital Univ. Hospital, CH-3010 Berne, Switzerland (E-mail: dominique.erni@insel.ch).

The costs of publication of this article were defrayed in part by the payment of page charges. The article must therefore be hereby marked "*advertisement*" in accordance with 18 U.S.C. Section 1734 solely to indicate this fact.

carriers with high oxygen affinity (11) may be beneficial for the oxygenation of hypoxic tissues, in which O_2 diffusion from oxygen carrier to tissue is ensured by the high gradient of Po_2.

The aim of this study was to test the effect obtained by increasing the oxygen affinity of HbVs on the oxygenation of the ischemic hamster flap tissue during normovolemic hemodilution with HbVs suspended in 6% Dx70. To this end, HbV with a P_{50} of 15 mmHg (HbV15) was compared with an HbV (P_{50} = 30 mmHg; HbV30) with an oxygen affinity similar to that of hamster blood (P_{50} = 28 mmHg). Furthermore, we wanted to evaluate the influence of the degree of normovolemic blood replacement with the HbV solutions. We chose a protocol that included three steps of hemodilution up to a level of 50% blood exchange, beyond which a clinical use does not appear to be reasonable.

MATERIALS AND METHODS

Experiments were performed according to the National Institutes of Health *Guidelines for the Care and Use of Laboratory Animals* and with the approval of the local Animal Ethics Committee. Thirty-seven male Syrian golden hamsters weighing 65–85 g were used in this study. The animals were randomly assigned to the control group (n = 9) or to one of three groups subjected to stepwise normovolemic hemodilution with 6% Dx70 (n = 10) or HbV15 or HbV30, respectively, suspended in 6% Dx70 (HbV15-Dx70, n = 9; HbV30-Dx70, n = 9).

Animal and flap preparation. The experiments were performed in a hamster skin flap model as described previously (4–6). Anesthesia was induced by pentobarbital injected intraperitoneally (100 mg/kg body wt, Nembutal, Abbott Laboratories; Chicago, IL). The carotid artery and jugular vein were cannulated for blood pressure monitoring and for the blood exchange and laboratory analysis, respectively. Catheterization and flap dissection were performed with the aid of an operating microscope at ×10 magnification (Wild; Heerbrugg, Switzerland). After the animal was shaved and the back skin of the animal was epilated, the vascular anatomy was identified by diaphanoscopy. An island flap measuring 30 × 20 mm was dissected free from the surrounding tissue. The animal was then placed in a lateral postition on a specially designed Plexiglas stage providing a platform for mounting the flap, which was positioned with the skin lying on the platform and kept at its original size by sutures. The panniculus carnosus was meticulously removed except for a single layer of muscle tissue left in place to protect the vascular network. The flap was merely perfused via one artery and vein, which bifurcate into two equal-sized branches within the flap, each of them supplying a separate vascular territory. One of the branches was transected after being secured with microsurgical ligatures. Therefore, one vascular territory was anatomically perfused by the intact branch, whereas the other was indirectly perfused through the collateral vasculature connecting the two vascular networks. The raw surface of the flap was finally covered with a polyvinyl film to isolate the tissue from the environment. During surgery, 4 mg papaverine hydrochloride (Sigma; St. Louis, MO) dissolved in 1 ml physiological saline solution was applied to the pedicle by a soaked cotton tip to prevent vascular spasm.

Laboratory analysis. Blood samples were collected in 40 μl heparin-washed microtubes for measurement of total Hb concentration and arterial blood gases (ABL 625, Radiometer; Copenhagen, Denmark). Hematocrit was determined by centrifugation.

Microhemodynamic measurements. Investigations were performed using an intravital microscope (Axioplan 1, Zeiss; Jena, Germany). Microscopic images were captured by a television camera (intensified charge-coupled device camera, Kappa Messtechnik; Gleichen, Germany), recorded on video (50 Hz, Panasonic; Osaka, Japan), and displayed on a television screen (Trinitron PVM-1454QM, Sony; Tokyo, Japan). The preparation was observed visually with a ×40 objective resulting in a total optical magnification of ×909 on the videomonitor. Microvascular diameter was measured by transillumination with a green filter, which gave a well-defined image of the width of the erythocyte column. For the assessment of centerline velocity, white blood cells (WBCs) were stained in vivo with rhodamine 6G (2 μmol/kg body wt iv, Sigma). Fluorescence was visualized with the aid of an excitation filter (530–560 nm), a dichroic mirror (580 nm), and a barrier filter (580 nm) and through epi-illumination by a mercury lamp (Atto Arc, Zeiss) (13). Velocity was calculated by measuring the distance covered by the WBC during one time frame (20 ms). Microvascular blood flow (Q) was calculated by means of *Eq. 1*

$$Q = \pi \times (\text{WBC velocity}/1.6) \times (\text{diameter}/2)^2 \qquad (1)$$

The value 1.6 represents the empirically determined ratio of centerline velocity to whole blood velocity (9).

The microvessels were classified according to physiological and anatomic features into conduit arterioles (connections to each other), end arterioles, and small venules (4, 12). The vessels were chosen for examination according to their optical clarity.

Tissue oxygen tension. Tissue Po_2 was assessed with Clark-type microprobes consisting of polarographic electrodes and an oxygen-sensitive microcell (Revoxode CC1, GMS; Kiel, Germany). According to the manufacturer, the Revoxode CC1 provides reproducible values for several consecutive days without the need of recalibration. The length of the cell was 1 mm, and the sampling area was within 1 mm of the cell. The probes were inserted into the subcutaneous tissue in the center of each vascular territory under visual control and microscopic magnification. Care was taken to place the probes in such a way that no arterioles or large venules lay within the sampling area.

Table 1. *Physicochemical characteristics of hamster blood and the diluents*

	Hamster Blood	Dx70	HbV15-Dx70	HbV30-Dx70
P_{50}, mmHg	28		15	30
Hill number	2.8		1.7	2.3
OTE, %	31		19	35
Oxygen capacity, ml/100 ml	24.3		9.1	9.1
[Hb], g/dl	17	0	7.5	7.5
[metHb], %			5.2	2.3
Oncotic pressure, mmHg	18	50	50	50
Viscosity, cP	4.5	2.8	8.7	8.7

HbV15-Dx70 and HbV30-Dx70, hemoglobin vesicles (HbVs) with a P_{50} of 15 mmHg (HbV15) and 30 mmHg (HbV30) suspended in 6% Dextran 70 (Dx70), OTE, oxygen transport efficiency (arteriovenous difference in oxygen saturation of Hb in hamsters); metHb, methemoglobin. Viscosity was measured at 37°C and at 150 s^{-1}.

Table 2. *MAP and laboratory data at baseline and during blood exchange*

	Baseline	Level of Blood Exchange		
		15%	30%	50%
Hematocrit				
Control	0.54 ± 0.05	0.53 ± 0.04	0.51 ± 0.03	0.51 ± 0.05
Dx70	0.51 ± 0.04	0.39 ± 0.05†	0.30 ± 0.06†	0.20 ± 0.05†
HbV15-Dx70	0.51 ± 0.07	0.41 ± 0.08†	0.32 ± 0.07†	0.22 ± 0.07†
HbV30-Dx70	0.56 ± 0.06	0.46 ± 0.05†	0.33 ± 0.06†	0.20 ± 0.03†
Total Hb concentration, g/dl				
Control	16.6 ± 1.0	16.3 ± 0.8	16.1 ± 0.7	16.0 ± 0.8
Dx70	16.7 ± 1.0	12.9 ± 1.7†	9.9 ± 2.0†	6.5 ± 1.5†
HbV15-Dx70	16.7 ± 2.1	14.2 ± 2.6†	11.7 ± 2.5†	8.7 ± 2.2†
HbV30-Dx70	18.1 ± 1.8	14.6 ± 1.3†	11.1 ± 1.2†	8.0 ± 1.0†
MAP, mmHg				
Control	87 ± 11	80 ± 8	83 ± 9	79 ± 5
Dx70	81 ± 7	81 ± 10	81 ± 8	79 ± 8
HbV15-Dx70	78 ± 7	81 ± 9	80 ± 8	78 ± 4
HbV30-Dx70	91 ± 8	90 ± 9	90 ± 9	86 ± 11
P_{O_2}, mmHg				
Control	47 ± 6	48 ± 7	45 ± 7	47 ± 8
Dx70	43 ± 10	49 ± 18	58 ± 19*	71 ± 17†
HbV15-Dx70	45 ± 8	47 ± 13	49 ± 14	53 ± 13
HbV30-Dx70	42 ± 7	47 ± 15	51 ± 14	52 ± 7*
P_{CO_2}, mmHg				
Control	62 ± 8	62 ± 9	62 ± 9	60 ± 8
Dx70	61 ± 5	59 ± 8	53 ± 8†	51 ± 7†
HbV15-Dx70	59 ± 6	56 ± 8	55 ± 8	53 ± 8
HbV30-Dx70	55 ± 4	52 ± 6	51 ± 5	50 ± 5
pH				
Control	7.23 ± 0.05	7.25 ± 0.06	7.25 ± 0.08	7.25 ± 0.09
Dx70	7.24 ± 0.04	7.24 ± 0.05	7.28 ± 0.05	7.30 ± 0.07
HbV15-Dx70	7.23 ± 0.05	7.25 ± 0.07	7.27 ± 0.06	7.30 ± 0.08
HbV30-Dx70	7.26 ± 0.05	7.27 ± 0.06	7.29 ± 0.05	7.29 ± 0.05

Values are means ± SD. MAP, mean arterial blood pressure. *$P < 0.05$ and †$P < 0.01$ vs. baseline.

HbV solutions. The HbVs were prepared as previously reported (22, 24). They consisted of isolated human Hb encapsulated in a phospholipid vesicle coated with polyethylene glycol. The size of the vesicles was 253 ± 63 nm. The oxygen affinity (P_{50}) was regulated by adding the coencapsulated allosteric effector pyridoxal 5′-phosphate, and it was calculated from the O_2 equilibrium curve measured with a Hemox Analyzer (TCS Medical Products) at 37°C (24). The HbVs were suspended in 6% Dx70 (B. Braun Medical; Emmenbrucke, Switzerland). The physical characteristics of the so-

Table 3. *Microhemodynamic data in anatomically perfused and ischemic tissue at baseline*

	Diameter, μm			Centerline Velocity, mm/s		
	Conduit arterioles	End arterioles	Venules	Conduit arterioles	End arterioles	Venules
			Anatomically perfused tissue			
Control	55 ± 18	6.5 ± 2.2	75 ± 18	7.3 ± 2.2	1.6 ± 0.8	2.1 ± 1.2
n	20	15	8	20	15	8
Dx70	52 ± 29	7.2 ± 2.6	88 ± 7	7.8 ± 3.0	3.0 ± 1.6	2.1 ± 1.1
n	19	29	9	19	29	9
HbV15-Dx70	53 ± 23	6.4 ± 1.7	83 ± 9	6.4 ± 2.7	1.9 ± 1.0	1.1 ± 0.4
n	13	23	7	13	23	7
HbV30-Dx70	52 ± 16	7.5 ± 1.8	86 ± 19	7.3 ± 2.6	2.2 ± 0.7	1.8 ± 0.8
n	25	16	17	25	16	17
			Ischemic tissue			
Control	56 ± 29	7.8 ± 3.4	83 ± 13	0.5 ± 0.4	0.3 ± 0.2	0.2 ± 0.0
n	18	21	10	18	21	10
Dx70	63 ± 34	8.3 ± 3.0	90 ± 11	0.8 ± 0.7	0.5 ± 0.3	0.4 ± 0.3
n	21	31	9	21	31	9
HbV15-Dx70	70 ± 31	6.7 ± 2.2	89 ± 13	0.4 ± 0.3	0.2 ± 0.1	0.2 ± 0.1
n	15	25	9	15	25	9
HbV30-Dx70	54 ± 20	8.6 ± 2.3	77 ± 16	0.7 ± 0.3	0.4 ± 0.2	0.2 ± 0.1
n	27	25	12	27	25	12

Values are means ± SD; *n*, sample size. Note that centerline velocity was significantly lower in the ischemic vessels than in the anatomically perfused vessels ($P < 0.01$).

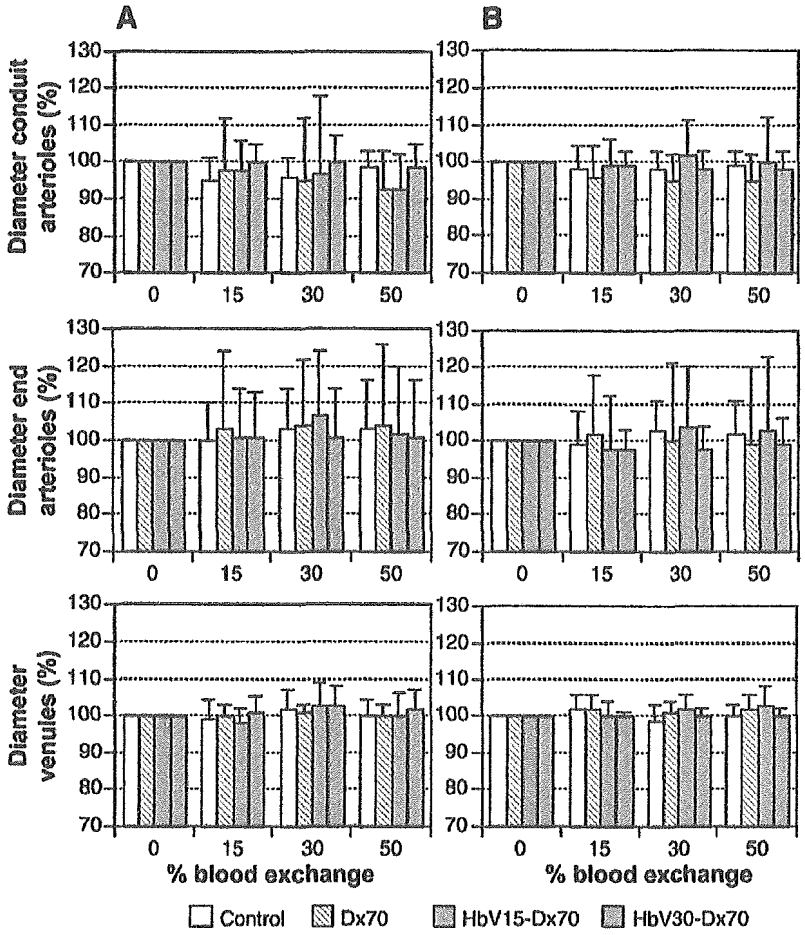

Fig. 1. Microvascular diameters in the anatomically perfused (*A*) and ischemic (*B*) tissues at baseline and after stepwise exchange of 15%, 30%, and 50% total blood volume with 6% Dextran 70 (Dx70) and Hb vesicles (HbVs) with a P_{50} of 15 mmHg (HbV15) and 30 mmHg (HbV30) suspended in Dx70. Data are given as a percentage of baseline and represent means ± SD.

lutions are summarized in Table 1. Oncotic pressure and viscosity were measured with a colloid osmometer (model 4420, Wescor; Logan, UT) and a cone-plate viscometer (PVII+, Brookfield Engineering; Middleboro, MA), respectively (30).

Protocol. The animals were kept under light anesthesia with a continuous infusion of 50 mg/ml pentobarbital given at a rate of ~0.5 mg·min^{-1}·kg body wt^{-1} throughout the experiment. The depth of anesthesia was regulated by tolerance of a noxious reflex due to pinching of the hind paw but no nonaversive reflexes (palpebral, corneal, and jaw reflex). A constant temperature in the animal and flap preparation was maintained by means of a heating pad and by keeping the room temperature at 28°C. Normovolemic hemodilution was achieved by simultanous replacement of withdrawn blood over 10 min. Hemodilution was performed in three steps at an interval of 1 h, thus reaching levels of 15%, 30%, and 50% of blood exchange. Measurements were taken at the end of each interval.

Inclusion criteria were a normal vascular anatomy, sufficient optical clarity of the preparation, and a mean arterial pressure above 60 mmHg.

The animals were euthanized with an overdose of pentobarbital at the end of the experiment.

Statistical analysis. The InStat version 3 program (Graph Pad Software, San Diego, CA) was utilized for statistical analysis. If the assumption of a normal distribution was appropriate, data were presented as means ± SD; otherwise, they represented median and 25th and 75th percentiles. For normally distributed data, the time-related differences between repeat measurements and the differences between the groups were assessed by the paired and unpaired ANOVA, respectively, whereas the nonparametric Friedman and Kruskal-Wallis tests were used for not normally distributed data analysis. All tests were followed by the Bonferroni post test. A value of $P < 0.05$ was taken to represent statistical significance.

RESULTS

Five animals (1 control, 1 Dx70, 1 HbV15-Dx70, and 2 HbV30-Dx70) did not fulfill the inclusion criteria and were excluded from this study.

The systemic data are summarized in Table 2. Similar hematocrits were obtained in all hemodiluted animals. After the 50% blood exchange, hemodilution with Dx70 resulted in a mean total Hb concentration of 6.5 g/dl, whereas the addition of HbV to the diluents enhanced the total Hb concentration to 8.7 and 8.0 g/dl, respectively ($P < 0.05$). Arterial P_{O_2} was gradually raised after each step of hemodilution, reaching 71 mmHg in the Dx70 group ($P < 0.01$ vs. baseline) and 53 and 52 mmHg for HbV15-Dx70 [not significant (NS)] and HbV30-Dx70 ($P < 0.05$), respectively (both $P < 0.05$ vs. Dx70). Furthermore, the blood exchange was followed by gradual reductions of arterial P_{CO_2} ($P <$

0.01 for Dx70; NS for the HbV groups) and increases in pH (NS).

At baseline, the microhemodynamic data were similar in all groups. The diameters and centerline velocities for conduit arterioles, end arterioles, and venules in each part of the flap are summarized in Table 3. Mean centerline velocities were significantly reduced in the ischemic vessels compared with the anatomically perfused vessels ($P < 0.01$).

The behavior of the microvascular diameters in both parts of the flap are shown in Fig. 1. A slight vasoconstriction was observed in the conduit arterioles after hemodilution with Dx70 (93 ± 10% in the anatomically perfused tissue and 95 ± 7% in the ischemic tissue, both NS) and HbV15-Dx70 (93 ± 9% anatomically perfused, NS), whereas the diameters remained virtually stable in the other microvessels in all groups.

Microvascular blood flow did not show any relevant changes in the anatomically perfused vessels (Fig. 2), whereas it was significantly increased in all vessels in the ischemic tissue due to hemodilution ($P < 0.05$ for Dx70 and HbV15-Dx70; $P < 0.01$ for HbV30-Dx70). The highest values were obtained with the 30% and 50% blood exchanges, reaching 144% (108–160%) for Dx70, 166% (152–192%) for HbV15-Dx70, and 141% (118–165%) for HbV30-Dx70.

Mean Po_2 ranged between 23.0 ± 4.3 and 26.7 ± 2.2 mmHg in the anatomically perfused tissue. Tissue Po_2 was significantly reduced in the ischemic part, where the values were between 7.7 ± 3.2 and 10.9 ± 3.4 mmHg ($P < 0.01$). In the anatomically perfused tissue, oxygenation was virtually not influenced by hemodilution with or without HbVs (Fig. 3). In the ischemic tissue, a transient improvement was observed during hemodilution with Dx70. The maximum was obtained after the 30% exchange (121 ± 17% of baseline, $P < 0.05$). Each step of blood exchange caused an increase in ischemic tissue oxygenation if the diluents contained HbV. Tissue Po_2 was enhanced up to 217 ± 67% and 164 ± 33% for HbV15-Dx70 and HbV30-Dx70, respectively (both $P < 0.01$ vs. baseline and other groups).

DISCUSSION

The principal findings of this study were that *1)* oxygenation in the ischemic, collateralized, and hypoxic flap tissue was raised with each step of hemodilution with both HbV solutions and that higher values

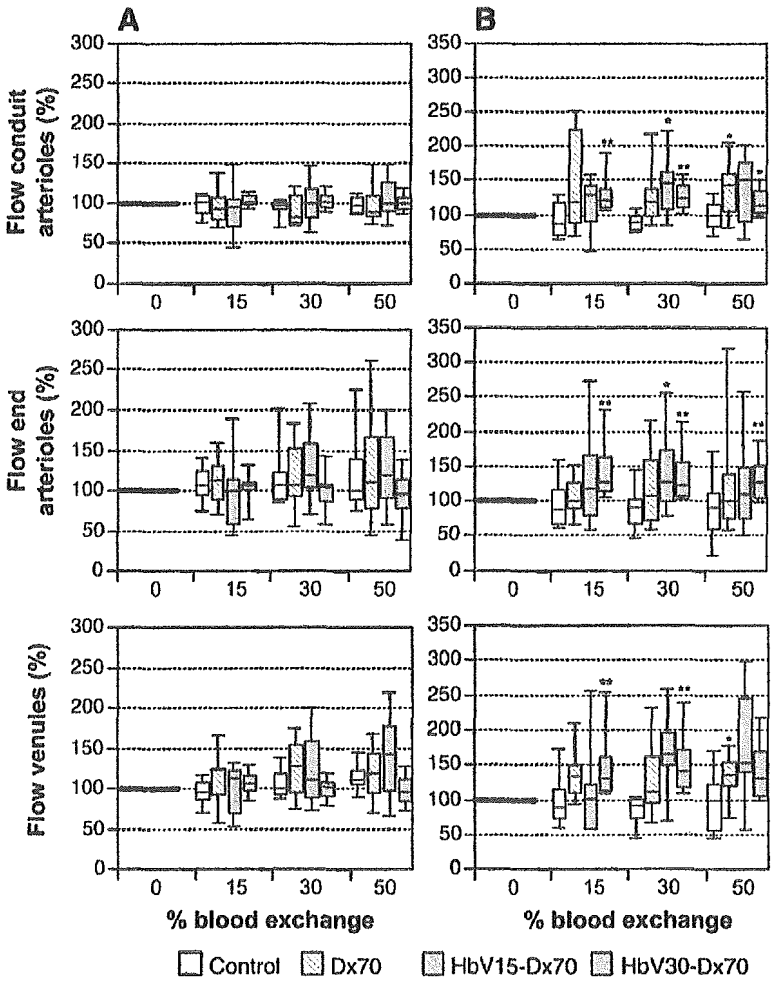

Fig. 2. Microvascular blood flow in the anatomically perfused (*A*) and ischemic (*B*) tissues at baseline and after stepwise exchange of 15%, 30%, and 50% total blood volume with 6% Dx70, HbV15-Dx70, and HbV30-Dx70. Data are given as a percentage of baseline and are presented in box plots reflecting 10th percentile, 25th percentile, median, 75th percentile, and 90th percentile. $*P < 0.05$ and $**P < 0.01$ vs. baseline.

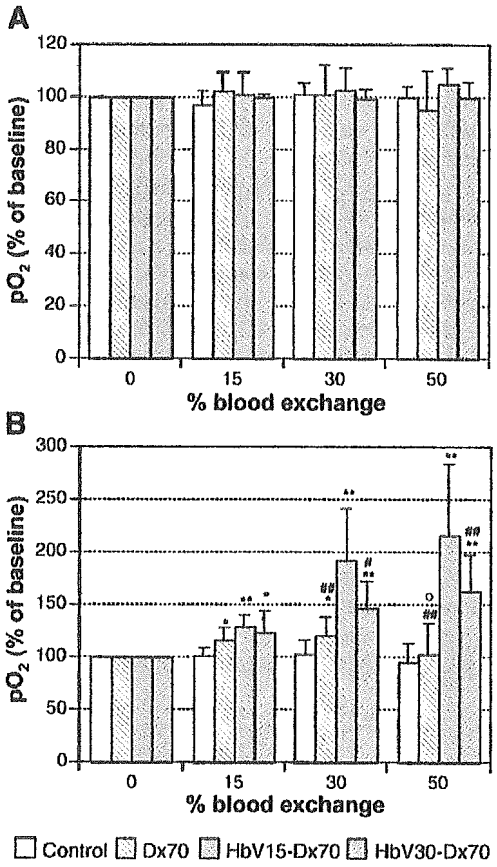

Fig. 3. Po_2 in the anatomically perfused (*A*) and ischemic (*B*) tissues at baseline and after stepwise exchange of 15%, 30%, and 50% total blood volume with 6% Dx70, HbV15-Dx70, and HbV30-Dx70. Data are given as a percentage of baseline and represent means ± SD. $^*P < 0.05$ and $^{**}P < 0.01$ vs. baseline; $\#P < 0.05$ and $\#\#P < 0.01$ vs. HbV15-Dx70; $^oP < 0.01$ vs. HbV30-Dx70.

were obtained *2*) by increasing the oxygen affinity of HbV and *3*) with HbV-containing solutions compared with Dx70 only.

Normovolemic hemodilution with Dx70 transiently improved the oxygenation in the ischemic tissue, reaching a peak of 121% of baseline at the 30% blood exchange. This level of hemodilution is considered to provide the highest RBC flux at the capillary level (15), thus resulting in maximal oxygen transport capacity both systemically (28) and in locally ischemic tissue (25). Furthermore, arterial Po_2 was increased at this level of hemodilution due to hyperventilation. As we (5) demonstrated in previous experiments in the same model, increased arterial Po_2 values were transferred as far as the collateral arterioles, which is where the blood circulation enters the ischemic tissue. In the present study, however, the improvement of oxygenation in the ischemic tissue was by far higher if HbV was added to the Dx70 solution, although microvascular blood flow, Hb concentration, and arterial Po_2 were similar or lower. Moreover, the oxygenation was enhanced despite a simultaneous decrease in total Hb concentration due to hemodilution with the HbV-Dx70 solutions. These results suggest that under the given conditions, the presence of HbVs increases the capacity of blood to deliver oxygen to the ischemic tissue and that the effect is related to the level of blood exchange with HbV solutions.

The effect may be achieved due to the small size of the HbVs, which might allow them to perfuse capillaries that are no longer accessible to RBCs due to intraluminal obstructions or reduced perfusion pressure that have to be assumed in the ischemic, collateralized tissue in the present model. Indeed, circulating HbVs could be observed in capillaries that were no longer considered functional because of the cessation of RBC flux (23). However, our previous experiments (6) showed that the improvement of oxygenation in the ischemic tissue obtained after hemodilution with HbV solutions was dependent on an increased RBC flux in this tissue, which indicates that mechanisms different from the passage of HbVs through vascular obstructions may be present.

On the basis of previous intravascular oxygen tension measurements, it was estimated that 40–50% of the systemic arterial oxygen content exited the upstream vasculature before reaching the collateralized, ischemic flap tissue (5, 24). It has been shown in both experimental (8, 24) and theoretical (31) studies that oxygen delivery may be delayed in favor of the downstream vasculature if oxygen carriers with increased oxygen affinity are infused. It is conceivable that this effect was responsible for the increased ischemic tissue oxygenation obtained with HbV15-Dx70 in our study. The high oxygen affinity of HbV15 did not seem to hamper the unloading of oxygen to this tissue, which is promoted by the high oxygen tension gradient and the increased residence time of circulating blood (11). Furthermore, it may be assumed that oxygen delivery is facilitated due to metabolic acidosis, thus causing a shift of the oxygen dissociation curve to the right.

The results obtained with HbV30-Dx70 suggest that prevention of oxygen loss in the upstream vasculature may have been accomplished without raising the oxygen affinity of HbV. It has been shown that the diffusion of oxygen through the plasma may substantially be influenced by adding oxygen carriers (14, 16, 17). According to the Stokes-Einstein equation, the diffusivity of oxygen is inversely proportional to the size of the plasma-bound oxygen carrier and the viscosity of the suspension. In mathematical models and in vitro experiments, facilitated oxygen diffusion was ascribed to small-sized Hbs (14, 16, 17, 21), whereas, because of their large size, this effect was abolished if HbVs were used (21). Although not measured in our study, there is sufficient evidence to assume a marked increase in viscosity of the plasma suspension obtained during hemodilution with the HbV-Dx70 solutions, because an increase in plasma viscosity from 1.2 to 1.4 cP has been observed in hamsters after severe hemodilution with Dx70 (30), which has a threefold lower viscosity than HbV-Dx70. Taken together, it may be assumed that hemodilution with the HbV-Dx70 solutions caused a retention of oxygen in the upstream vasculature, which